

**Real-Time QRS Detection Using Wavelet Packet Transform**

Wisarut Bholsithi\*, Surapun Yimman\*, Watcharapong Hinjit\* and Kobchai Dejhan\*\*

\* Department of Industrial Physic & Medical Instrumentation,  
King Mongkut’s Institute of Technology North Bangkok, Bangkok, 10800, Thailand  
(Tel : +66-2-913-2500; E-mail: sym@kmitnb.ac.th, wisarut.bholsithi@nectec.or.th)

\*\*Faculty of Engineering and Research Center for Communication and Information Technology,  
King Mongkut’s Institute of Technology Ladkrabang, Bangkok, 10520, Thailand

**Abstract:** The wavelet packet transform has been applied for QRS detection with squaring, window integration, and impulse filter techniques to cut down the false detection of QRS complex. This real time QRS detection has been performed on Simulink and Matlab. The correct QRS detection rates have reached to 99.75% in the experiment with 15 sets of ECG data from European ST-T database which are kept in Physionet.

**Keywords:** Wavelet Packet Transform, Real time QRS Detection, ECG analysis system, Simulink, Matlab

**1. INTRODUCTION**

QRS detection is the basic building block for ECG analysis system, and the accurate QRS detection is the most critical element for ECG analysis since the false detection of QRS complex will consume the memory for ECG analysis system, and cause erroneous interpretation of ECG waves during the analysis. Faster QRS detections will enable the physicians as well as the ECG analysis system to response to the patients on time. [1, 2, 3, 5, 7]

There are several types of QRS detectors available including Wavelet transforms [2]. However, wavelet transform has limited bands for filtering ECG signals before detecting QRS complex. Therefore, the researchers have applied the wavelet packet as the ways to make more wavelet filter bands available for QRS detections.

**2. METHODS**

**2.1 Wavelet Packet Transform**

Wavelet packet transform of signal  $f(x)$  is defined as:

$$\psi_{j+1}^{2p}(t) = \sum_{n=-\infty}^{\infty} h[n]\psi_j^p(t - 2^j n) \tag{1}$$

$$\psi_{j+1}^{2p+1}(t) = \sum_{n=-\infty}^{\infty} g[n]\psi_j^p(t - 2^j n) \tag{2}$$

Where

$\psi_j^p(t)$  is wavelet packet at scale  $j$  and binary tree  $p$ th branch,  $0 \leq p \leq 2^j - 1$

$h[n]$  is low-pass wavelet packet filter coefficients which is equal to the following expression:

$$h[n] = \langle \psi_{j+1}^{2p}(u), \psi_j^p(u - 2^j n) \rangle \tag{3}$$

$g[n]$  is high-pass wavelet packet filter coefficients which is equal to the following expression:

$$g[n] = \langle \psi_{j+1}^{2p+1}(u), \psi_j^p(u - 2^j n) \rangle \tag{4}$$

The parent node is divided in 2 orthogonal subspaces as shown in Fig. 1 and  $W_{p,j}$  will be the result after the convolution of signal with  $\psi_j^p(t)$ .

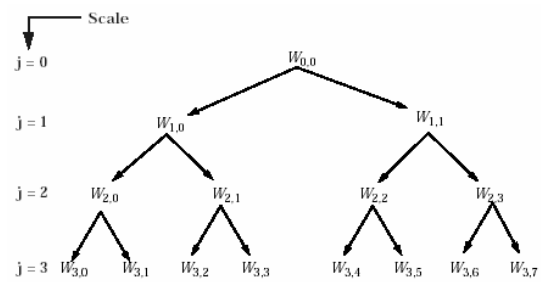


Fig. 1 Binary tree of Wavelet Packet Spaces

**2.2 Detecting QRS Complex with Wavelet Packet Transform**

The wavelet used in this experiment is the quadratic spline wavelet originated by Mallat since it has the singularity detection properties. There are a few families of wavelet transform which have edge detection properties such as the derivatives of Gaussian function [3, 4], Haar wavelet [7], Morlet wavelet and so on.

The reason for this selection is that the quadratic spline wavelet has both wavelet function and scaling function while derivative of Gaussian function and Morlet wavelet have only wavelet function. The coefficients of quadratic spline wavelet filters at the first decomposition level originated by [8] can be shown in Table 1.

Table1 Wavelet filter Coefficients

N	$\frac{h[n]}{\sqrt{2}}$	$\frac{\hat{h}[n]}{\sqrt{2}}$	$\frac{g[n]}{\sqrt{2}}$	$\frac{\hat{g}[n]}{\sqrt{2}}$
-2				-0.03125
-1	0.125	0.125		-0.21875
0	0.375	0.375	-0.5	-0.6875
1	0.375	0.375	0.5	0.6875
2	0.125	0.125		0.21875
3				0.03125

ECG signal into the 1<sup>st</sup> derivative of the original signal which QRS complex, T waves and P waves will become series of modulus maxima pairs after applying wavelet filter. The 1<sup>st</sup> level of wavelet decomposition will be displayed in Fig. 2 while the 2<sup>nd</sup>, the 3<sup>rd</sup>, and the 4<sup>th</sup> level of decomposition will be shown from Figs. 3 to 5, respectively. At the 5<sup>th</sup> page, it has been divided into 2 sections according to the first decomposition level–section (a) for the low pass filter  $h[n]$  vs. and section (b) for the high pass filter  $g[n]$ .

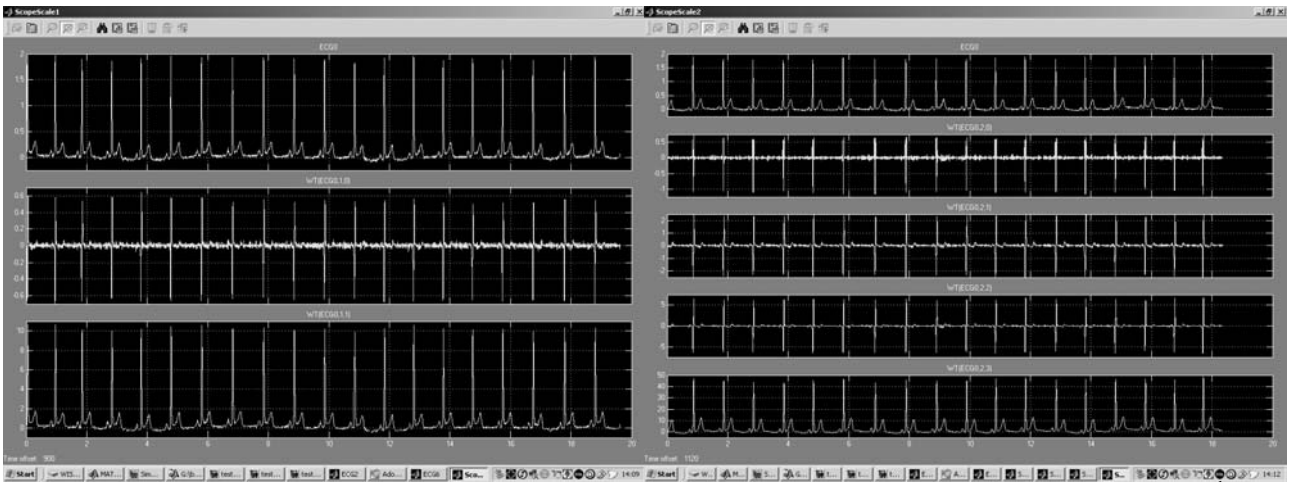


Fig. 2 Wavelet Packet Decomposition at the 1<sup>st</sup> Level for ECG0 from E0103.

Fig. 3 Wavelet Packet Decomposition at the 2<sup>nd</sup> Level for ECG0 from E0103.

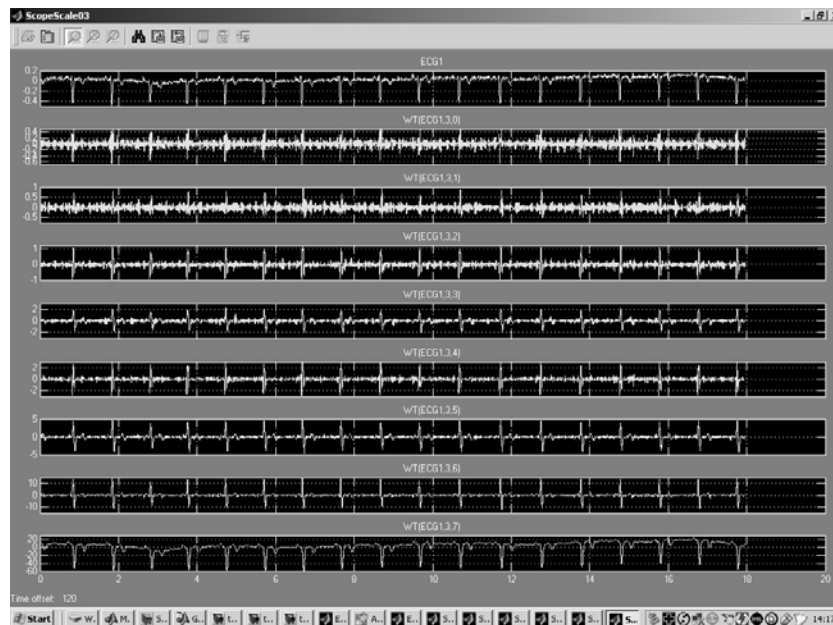
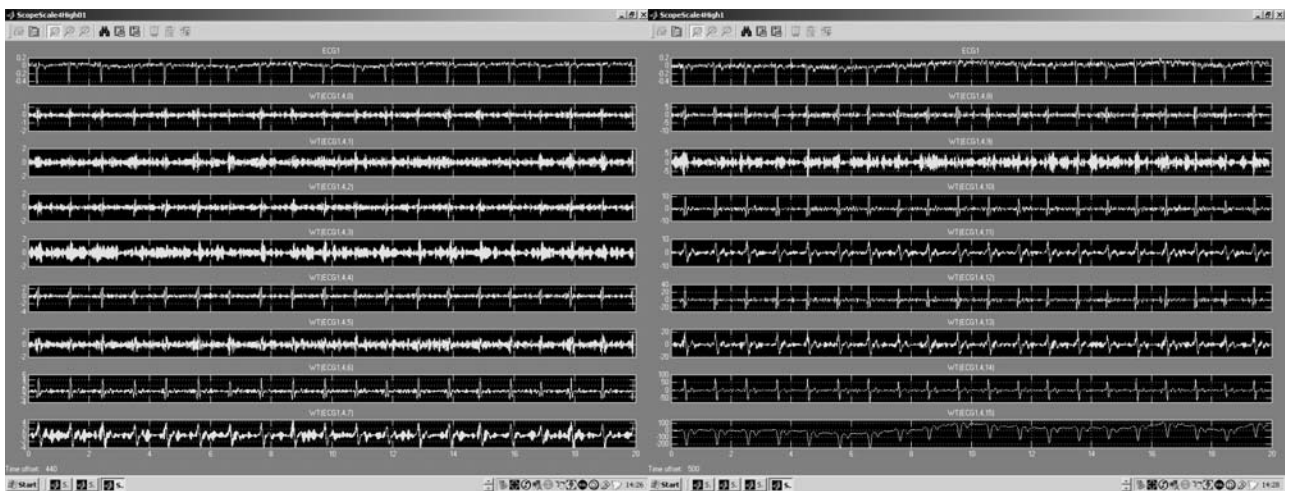


Fig. 4 Wavelet Packet Decomposition at the 3<sup>rd</sup> Level for ECG0 from E0103.



(a) (b)  
 Fig. 5 Wavelet Packet Decomposition at the 4<sup>th</sup> Level for ECG0 from E0103  
 (a)  $W_4^{2p}$  starting with HPF  $g[n]$  (b)  $W_4^{2p+1}$  starting with LPF  $h[n]$

For the case of QRS detection, researchers need to choose the wavelet packet filter that has the band closest to the QRS complex power spectrum as shown in Fig. 6. At that page, the QRS complex band is within the band of 5 – 15 Hz.

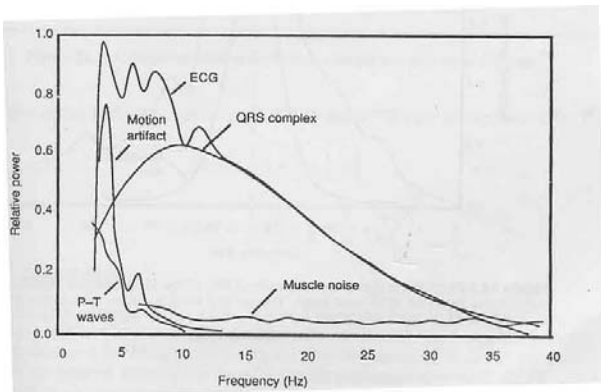


Fig. 6 ECG Power spectrum

From experiment, the researchers have found that the wavelet packet subspace 1 ( $p = 1$ ) of level 3 decomposition ( $j = 3$ ) will have a bandwidth closest to the bandwidth of QRS Complex as shown in Fig. 7 and the cutoff frequencies of the wavelet packet filters in scale 3 will be shown in Table 2 respectively.

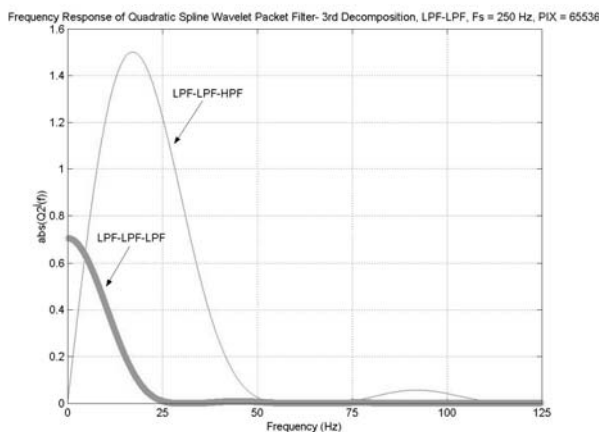


Fig. 7 Wavelet Packet Spectrum at branch  $p = 1$  (LPF-LPF-HPF) and  $p = 0$  (LPF-LPF-LPF) of the composition level  $j = 3$ .

Table 2 Cutoff Frequency of Wavelet Packet at the 3<sup>rd</sup> Decomposition Level (Only for the BPF sections which have the highest amplitude)

Wavelet Filters	Cutoff Frequency ( $f_{co}$ ) – Herz		
	$f_{Low}$	$f_{Peak}$	$f_{High}$
LPF-LPF-LPF ( $W_{3,0}$ )	8.2493	-	-
LPF-LPF-HPF ( $W_{3,1}$ )	8.3618	10.5076	27.4620
LPF-HPF-LPF ( $W_{3,2}$ )	50.1461	58.4145	67.0738
LPF-HPF-HPF ( $W_{3,3}$ )	68.4280	76.0231	85.9070
HPF-LPF-LPF ( $W_{3,4}$ )	116.6286	-	-
HPF-LPF-HPF ( $W_{3,5}$ )	96.3516	107.0080	116.2281
HPF-HPF-LPF ( $W_{3,6}$ )	55.0365	63.9744	72.7539
HPF-HPF-HPF ( $W_{3,7}$ )	76.0956	88.6402	101.7570

The wavelet packet subspace 3 ( $p = 3$ ) of level 4 decomposition ( $j = 4$ ) is another suitable filter for QRS detection. Fig. 8 will show band of wavelet packet decomposition level 4 at  $p = 2, 3$ .

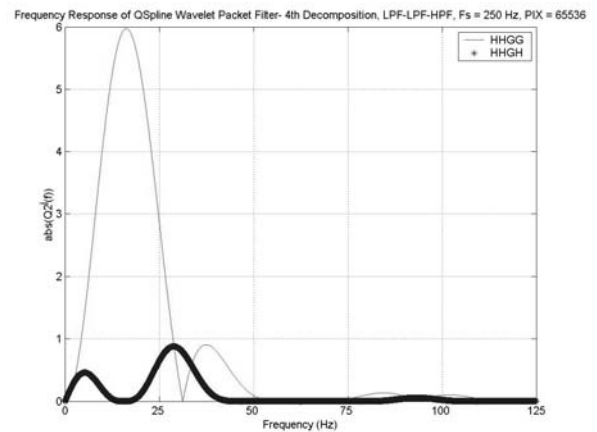


Fig. 8 Wavelet Packet Spectrum at branch  $p = 2$  (HHGH) and  $p = 3$  (HHGG) of the decomposition level  $j = 4$ .

At the same time, the wavelet packet decomposition level 4 ( $j = 4$ ) and the wavelet packet subspace 1 ( $p = 1$ ) is a suitable choice the detection of P wave and T Wave only after substituting the QRS complex section of ECG signals with isoelectric level. The band of wavelet packet decomposition level 4 at  $p = 0, 1$  is shown in Fig. 9.

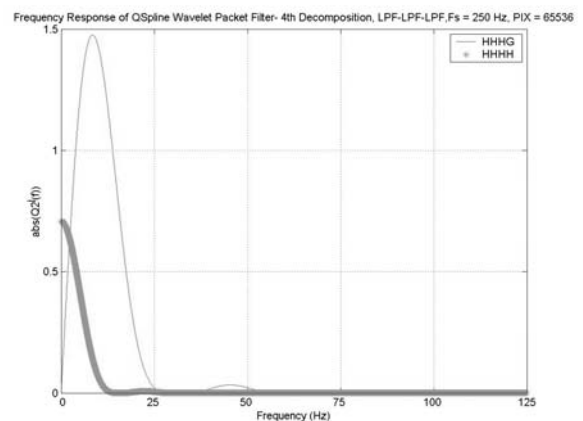


Fig. 9 Wavelet Packet Spectrum at branch  $p = 0$  (HHHH) and  $p = 1$  (HHHG) of the decomposition level  $j = 4$ .

The cutoff frequencies of the wavelet packet filters in scale 4 will be shown in Table 3 with red-highlighted data for QRS complex detection and the blue italic data for P Wave and T wave detection respectively while taking filter delays into account for accurate detection.

### 2.3 Implement Methods

Initially, researchers using wavelet filter to turn the ECG signal into series of modulus maxima pairs. After that, squaring the filter signal and then performing the window integration with the following equation

$$y(n) = [x(n)]^2 \quad (4)$$

$$y(n) = \frac{1}{N} \sum_{i=0}^{N-1} x(n-i) \quad (5)$$

The choice of window width depends upon the number of samples  $N$  corresponding to the width of QRS complex. The

width of QRS complex for defining the value of N should not be too large to cause QRS complex and T wave to merge and not be too small to cause multiple peaks corresponding to a single QRS complex. Sampling rate  $f_s$  of signal is another factor which influences the number of sample for window integration since the faster sampling rate will require higher number of samples for window integration. Therefore, the equation for finding N is:

$$N = f_s T_{QRS} \quad (6)$$

In this experiment, the QRS complex width  $T_{QRS}$  of choice will be 160 msec [10] which corresponding to the maximum width of QRS complex when there is a complete heart block which cause the delay of QRS complex and the sampling rate of signal is 250 Hz.

To cut down the false detections, it is necessary to apply the following methods for QRS detection [1,10]

1. If the detected pulses following QRS complex are less than 360 msec, they will be ignored.
2. Using the results from integrators as the threshold.
3. Threshold for QRS detection must be varying according to the ECG signals which user can readjust.
4. If the integrated value exceed the designated value (e.g.  $y[n] > 50$ ), cap the integration value to the designated value to

prevent data overflow ( $y[n] = 50$ ).

Table 3 Cutoff Frequency of Wavelet Packet at the 4<sup>th</sup> Decomposition Level (Only for the BPF sections which have the highest amplitude)

Wavelet	Cutoff Frequency ( $f_{co}$ ) Hz		
	$f_{Low}$	$f_{Peak}$	$f_{High}$
LPF-LPF-LPF-LPF ( $W_{4,0}$ )	4.1027	-	-
<b>LPF-LPF-LPF-HPF (<math>W_{4,1}</math>)</b>	<b>4.1122</b>	<b>8.4496</b>	<b>13.5288</b>
LPF-LPF-HPF-LPF ( $W_{4,2}$ )	24.7707	28.8315	33.1230
<b>LPF-LPF-HPF-HPF (<math>W_{4,3}</math>)</b>	<b>10.2692</b>	<b>16.2773</b>	<b>22.4628</b>
LPF-HPF-LPF-LPF ( $W_{4,4}$ )	57.4684	61.5482	65.7196
LPF-HPF-LPF-HPF ( $W_{4,5}$ )	47.0448	52.3567	57.2243
LPF-HPF-HPF-LPF ( $W_{4,6}$ )	27.1130	31.5266	35.9192
LPF-HPF-HPF-HPF ( $W_{4,7}$ )	37.0636	42.9058	49.3832
HPF-LPF-LPF-LPF ( $W_{4,8}$ )	-	-	120.8878
HPF-LPF-LPF-HPF ( $W_{4,9}$ )	99.8344	116.4627	124.9256
HPF-LPF-HPF-LPF ( $W_{4,10}$ )	91.6061	95.9225	100.0347
HPF-LPF-HPF-HPF ( $W_{4,11}$ )	102.2110	108.4251	114.5267
HPF-HPF-LPF-LPF ( $W_{4,12}$ )	88.7814	93.1721	97.6238
HPF-HPF-LPF-HPF ( $W_{4,13}$ )	74.6288	81.1749	87.3089
HPF-HPF-HPF-LPF ( $W_{4,14}$ )	58.6414	62.8262	66.9804
HPF-HPF-HPF-HPF ( $W_{4,15}$ )	67.1749	71.8803	77.2133

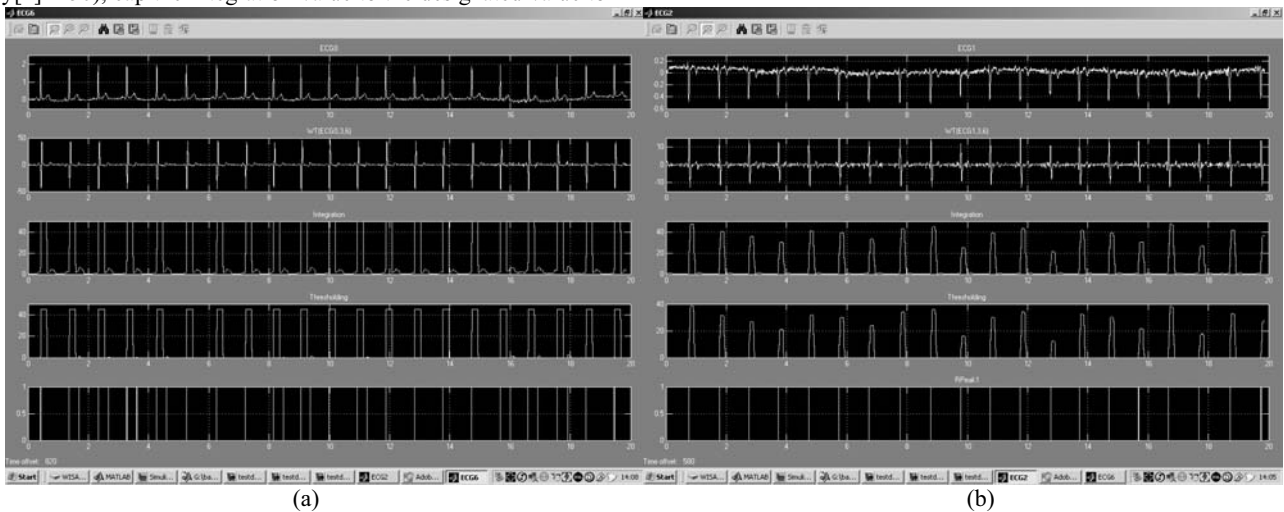


Fig. 10 Results from QRS Detection Algorithm  
(a) ECG0 as input (b) ECG1 as input

### 3. RESULTS

The detection program has been written in Simulink and m-files from MATLAB6.1® which have been used by [5, 6]. The researchers have used 15 sets of data at the first 20-minute interval (300,000 samples) from European ST-T database [12] to make a quantitative assessment on Wavelet packet algorithm.

Each full set of data European ST-T database will consist of a data file, an annotation file with the positions of QRS complex as well the positions important events relating with ECG data files, and a header file which contain brief information of the patient as well as a brief description of the data set. Each data file will contain 2 ECG signal and the time with the duration for each signal of 2 hour and sample rate of 250 Hz. The simulation results from QRS detection of ECG0 and ECG1 from E0103 data set will be shown in Fig. 10 (a) and (b) respectively.

On the other hand, the statistical results have been shown on Table 4 which FP referring to false positive data, FN referring to false negative data, Se referring to selectivity, +P

referring to Positive predictability, and DER referring to .

The false positive values (FP) are prominent in both ECG0 and ECG1 data from E0509, E0601 and E0615 dataset which are the case of patients with coronary artery disease and myocardial infarction with premature ventricular contraction (PVC). Inappropriate threshold readjustment at too low levels and the imperfect algorithm to filter impulses corresponding to T wave are other sources false positive data. The 360 msec thresholding is also too small since the 360 msec threshold has been started from the position of R wave, not the beginning of QRS complex as the researcher have done.

False negative data are prominent in ECG1 of E0119 data set which is the case of coronary artery with noise. Inappropriate threshold readjustment at too high level along with imperfect algorithm to filter impulses corresponding to T wave while preserving the impulse corresponding to QRS complex also other sources of the false negative problem [13].

#### 4. CONCLUSION AND FUTURE DEVELOPMENTS

This QRS complex detection is working with high percentage of QRS detection. However, the system needs improvement by setting up the QRS complex detection system, which takes the average recent average RR intervals into account to readjust the thresholds as real time QRS detection originated by [1] and modified source code in C as shown in [10]. After algorithm modification, the researchers could set up the additional systems to find the onset and offset of QRS complex, replace QRS complex section in the filtered data with isoelectric level to find T wave and P wave. After that, the researchers will set up additional system to locate the corresponding onsets and offsets of T wave and P wave for ECG analysis system later as the process shown in [11].

#### REFERENCES

- [1] J. Pan, and W.J. Thompkins, "Real time QRS Detection Algorithm," *IEEE Trans. BME.*, Vol.32, No.3, pp. 230-236, Mar. 1985.
- [2] C. Li, Zheng C., and Changfeng T., "Detection of ECG Characteristic Points Using Wavelet Transforms," *IEEE Trans. BME.*, Vol.42, No.1, pp. 22-28, Jan. 1995.
- [3] J.S. Sahambi, S.N. Tandon, and R.K.P. Bhatt, "Using Wavelet Transform for ECG Characterization, An Online Digital Signal Processing," *IEEE Eng. in Med. & Bio.*, pp. 77-83, Jan.-Feb. 1997
- [4] J.S. Sahambi, S.N. Tandon, and R.K.P. Bhatt, "An Automated Approach to Beat by beat QT Interval Analysis," *IEEE Eng. in Med. & Bio.*, pp.97-101, May-Jun. 2000
- [5] U. Kunzmann et. al., "Parameter Extraction of ECG Singals in Real-Time," *Biomedizinische Technik 47, Ergänzungsband 2*, pp. 534-537, 2002
- [6] G. von Wagner et. al, "Simulation Method for the Online Extraction of ECG Parameters under Matlab®/Simulink®," *Biomedizinische Technik 47, Ergänzungsband 2*, pp. 875-878, 2002
- [7] S. Wong et. al, "QT Interval Time-Frequency Analysis using Haar Wavelet," *IEEE Comp. In Cardiology*, pp. 405-408, 1998.
- [8] S. Mallat, and S.F. Zhong, "Characterization of Signals from Multiscale Edge," *IEEE Trans. PAMI*, Vo.14, No. 7, pp. 710-732, July 1992.
- [9] S. Mallat, *A Wavelet Tour of Signal Processing*, 2nd Edition, Academic Press, London, UK, pp. 322-339, 1998
- [10] W.J. Tompkins ed., *Biomedical Digital Signal Processing: C Language Examples and Laboratory Experiments for the IBM® PC*, Prentice-Hall International Inc., Englewood Cliffs, NJ, USA, pp. 236-264 1993
- [11] R.M. Rangayyan., *Biomedical Signal Analysis: A Case-Study Approach*, Wiley-Interscience, John Wiley & Sons, Inc., NY, USA, pp. 177-235, 2002
- [12] <http://www.physionet.org/physiobank/database/edb/>
- [13] <http://www.physionet.org/physiobank/annotations.shtml>

Table 4 Result from QRS Detection Algorithm

ECG Signal Set	No. of QRS	FP	FN	Se (%)	+P (%)	DER (%)	
E0103	ECG0	1366	0	1	100	99.927	0.0732
	ECG1	1366	0	1	100	99.927	0.0732
E0105	ECG0	1104	2	2	99.819	99.819	0.3623
	ECG1	1104	1	1	99.909	99.909	0.1812
E0111	ECG0	1213	1	0	99.918	100	0.0824
	ECG1	1213	1	0	99.918	100	0.0824
E0113	ECG0	1253	1	1	99.920	99.920	0.1596
	ECG1	1253	0	0	100	100	0
E0115	ECG0	1808	1	2	99.945	99.889	0.1659
	ECG1	1808	1	0	99.945	100	0.0553
E0119	ECG0	1212	1	1	99.918	99.917	0.1650
	ECG1	1212	4	18	99.670	98.532	1.8152
E0121	ECG0	1525	0	0	100	100	0
	ECG1	1525	0	0	100	100	0
E0123	ECG0	1533	0	0	100	100	0
	ECG1	1533	1	1	99.935	99.935	0.1305
E0125	ECG0	1450	0	0	100	100	0
	ECG1	1450	2	2	99.862	99.862	0.2759
E0139	ECG0	1569	0	0	100	100	0
	ECG1	1569	0	0	100	100	0
E0147	ECG0	1085	4	0	99.631	100	0.3687
	ECG1	1085	6	0	99.447	100	0.5530
E0151	ECG0	1135	2	1	99.824	99.912	0.2643
	ECG1	1135	4	2	99.648	99.823	0.5286
E0509	ECG0	1366	4	1	99.707	99.927	0.3660
	ECG1	1366	6	2	99.561	99.853	0.5857
E0601	ECG0	1149	10	0	99.123	100	0.8703
	ECG1	1149	14	7	98.782	99.387	1.8277
E0615	ECG0	1263	8	0	99.367	100	0.6334
	ECG1	1263	15	1	98.812	99.920	1.2668
Total/Average		40062	89	44	99.882	99.756	0.3629